JOURNAL OF BACTERIOLOGY, Apr. 2006, p. 3110–3115 Vol. 188, No. 8
0021-9193/06/$08.00+0 doi:10.1128/JB.188.8.3110–3115.2006

NOTES

EspF of Enteropathogenic *Escherichia coli* Binds Sorting Nexin 9

Oliver Marchès,[1] Miranda Batchelor,[1] Robert K. Shaw,[3] Amit Patel,[4] Nicola Cummings,[4] Takeshi Nagai,[5] Chihiro Sasakawa,[5] Sven R. Carlsson,[6] Richard Lundmark,[6] Celine Cougoule,[1,2] Emmanuelle Caron,[1,2] Stuart Knutton,[3] Ian Connerton,[4] and Gad Frankel[1]*

Division of Cell and Molecular Biology[1] and Centre for Molecular Microbiology and Infection,[2] Imperial College London, London SW7 2AZ, United Kingdom; Institute of Child Health, University of Birmingham, Birmingham B4 6NH, United Kingdom[3]; Division of Food Sciences, School of Biosciences, University of Nottingham, Loughborough LE 12 5DR, United Kingdom[4]; Department of Microbiology and Immunology, Institute of Medical Science, University of Tokyo, 4-6-1 Shirokanedai, Minato-ku, Tokyo 108-8639, Japan[5]; and Department of Medical Biochemistry and Biophysics, Umea University, S-901 87, Umea, Sweden[6]

Received 25 November 2005/Accepted 6 February 2006

EspF of enteropathogenic *Escherichia coli* targets mitochondria and subverts a number of cellular functions. EspF consists of six putative Src homology 3 (SH3) domain binding motifs. In this study we identified sorting nexin 9 (SNX9) as a host cell EspF binding partner protein, which binds EspF via its amino-terminal SH3 region. Coimmunoprecipitation and confocal microscopy showed specific EspF-SNX9 interaction and non-mitochondrial protein colocalization in infected epithelial cells.

Subversion of host cell physiology and homeostasis is the hallmark of enteropathogenic *Escherichia coli* (EPEC) infections (6). In particular, while colonizing the gut epithelium, EPEC modulates the actin (13), microtubule (9, 16, 24, 25), and intermediate filament (1, 27) networks, a process that leads to formation of distinct histopathological lesions termed "attaching and effacing" (A/E) (14). A/E lesions are characterized by effacement of brush border microvilli and intimate attachment of the EPEC bacterium to the plasma membrane of infected enterocytes. In addition, infected cells produce elongated actin-rich pedestal-like structures at the site of intimate bacterial adhesion (5).

The EPEC genes encoding A/E lesion formation and actin polymerization map to a pathogenicity island termed the locus of enterocyte effacement (LEE) (17), which encodes transcriptional regulators, the adhesin intimin, structural components of a type III secretion system, chaperones, translocators, and the effector proteins EspG, EspZ, EspH, Tir, Map, and EspF; other effector proteins are encoded by genes carried on prophages and small pathogenicity islands (6).

Several functions have been linked with specific LEE effectors. Map promotes rapid filopodium formation in a Cdc42-dependent manner (12). EspG binds tubulins and causes destabilization of the microtubule network (9, 16, 24, 25). EspH is a modulator of the host actin cytoskeleton affecting filopodium and pedestal formation (26). Tir (11) is targeted to the plasma membrane, where it adopts a hairpin loop topology (10); the extracellular domain of Tir binds intimin while the intracellular amino and carboxy termini interact with a number of focal adhesion and cytoskeletal proteins linking the extracellular bacterium to the cell cytoskeleton (8).

EspF has a major role in disruption of intestinal barrier function, being required for the loss of transepithelium resistance, for increased monolayer permeability, and for redistribution of the tight junction-associated protein occludin (19). Like Map, EspF is targeted to host mitochondria via its N-terminal region and is involved in mitochondrial membrane permeabilization. Moreover, it induces release of the toxic protein cytochrome *c* into the cytosol and cleavage of caspases 9 and 3, indicating that EspF plays a role at the beginning of the mitochondrial death pathway (2, 21, 22). Additionally, at early time points postinfection EspF forms a complex with cytokeratin 18 and the adaptor protein 14-3-3 (zeta isoform), a complex that is dismantled at later stages (27). Recent studies using human intestinal in vitro organ cultures have shown that EspF plays a direct role in remodeling brush border microvilli (23).

$EspF_{EPEC}$ contains three proline-rich repeats and six putative Src homology 3 (SH3) domain binding motifs (PxxP). Accordingly we hypothesized that EspF interacts with a host cell protein containing an SH3 domain. The aim of this study was to identify the host cell binding partner protein of EspF. To this end we performed a global *Saccharomyces cerevisiae* (strain PJ-69A) two-hybrid screen using EspF as bait (pICC175) (Table 1) and a human cDNA library as prey. RNA was prepared from HeLa cell cultures, and polyadenylated RNAs were selected using the poly(A) Quick mRNA isolation kit (Stratagene). Oligo$(dT)_{25}$ (dA/dC/dG) was used to prime first-strand cDNA synthesis by Moloney murine leukemia virus reverse transcriptase, and second-strand synthesis utilized a mixture of T4 DNA polymerase and RNase H. The cDNAs

* Corresponding author. Mailing address: Flowers Building, Imperial College London, London SW7 2AZ, United Kingdom. Phone: 44 (0)20 75945253. Fax: 44 (0)20 75945253. E-mail: g.frankel@imperial.ac.uk.

TABLE 1. Plasmids used in this study

Plasmid	Description	Reference
pICC175	pGBT-EspF	3
pICC347	Original clone containing truncated SNX9 gene in pGAD-GH	This study
pICC348	pGAD424 encoding $SNX9_{\Delta SH3}$	This study
pICC350	pET28a encoding His-EspF	This study
pICC351	pMAL-c2 encoding MBP-$SNX9_{214}$ fusion protein	This study
pICC352	pMAL-c2 encoding MBP-$SNX9_{\Delta SH3}$ fusion protein	This study
pKD46	Helper plasmid	4

TABLE 2. PCR primers

Primer	Sequence
SNX9-R	CGGGATCCTTACTGTTCCGTGCCAGG
SNX9-ΔF	GGAATTCGATGGAAAAGATCAATTTTCTTG
EspF-Fwd	AAGAATTCCTTAATGGAATTAGTAACGCT
SNX9-F	AAGGATCCTTACCCTTTCTTCGATTGCT
EspF-ΔF	ATGCTTAATGGAATTAGTAACGCTGCTTCT ACACTAGGGCGGCAGCTTGTTGTGTAGG CTGGAGCTGCTTCG
EspF-ΔR	TTACCCTTTCTTCGATTGCTCATAGGCAGCT AAATGATCTTTTAGTGCCTCATATGAATA TCCTCCTTAG

were ligated to an EcoRI-adapted linker and cloned into pGAD-GH (Clontech). The pGAD-GH cDNA clones were amplified in *E. coli* SURE (Stratagene) before plasmid DNA was transformed into yeast (PJ69-4A) as described previously (1). Following growth of the cotransformants under conditions that select for protein interactions, prey plasmids were rescued from all emerging clones and retransformed into PJ-69A with or without pICC175. Analysis of the cDNA inserts of plasmids that conferred growth on selective media only in the presence of EspF revealed that sorting nexin 9 (SNX9) is a potential new EspF partner protein.

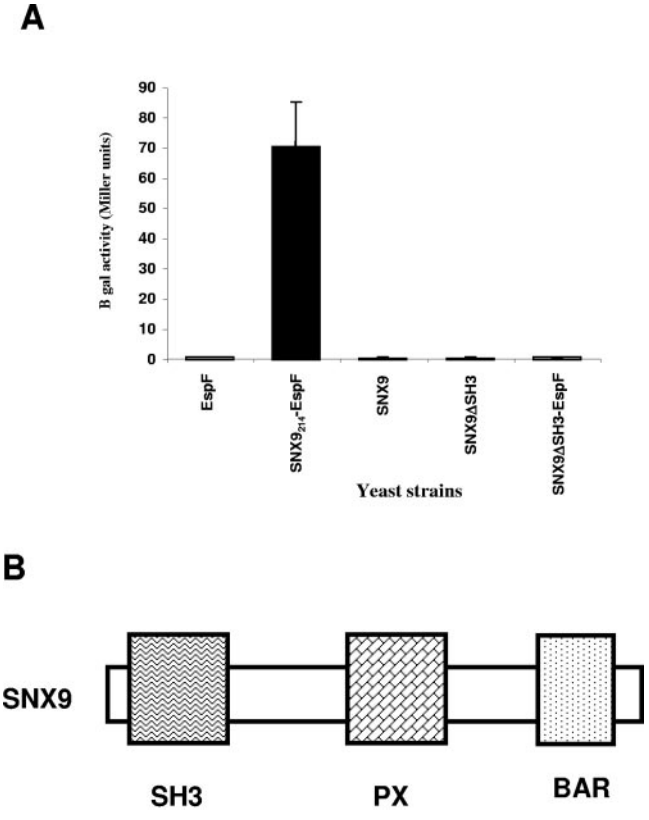

FIG. 1. A. Identification of SNX9 as an EspF target protein. Yeast containing pICC175 (encoding EspF) and pICC347 (encoding SNX9) demonstrated a ca. 35-fold increase in β-galactosidase activity compared to single-plasmid-bearing strains. Coexpression of EspF and SNX9ΔSH3 did not activate the β-galactosidase reporter gene. B. Schematic domain organization of SNX9 (not to scale).

The function of the nonselective reporter LacZ was assessed in the yeast strains by measuring β-galactosidase activities. Activation of the *lacZ* reporter was assessed by quantification of β-galactosidase activity in cell extracts (20). In each case, activation of *lacZ* was determined in triplicate for three colonies. While low levels were detected in the host or single-plasmid-bearing strains, a 35-fold increase was observed in the strain expressing EspF and SNX9 (PJ69-4A pICC175-pICC347) (Fig. 1A).

SNX9 binds EspF via its SH3 domain. Sequencing of the entire SNX9 cDNA clone (pICC347) revealed that it contains a truncated SNX9 gene, encoding only the N-terminal 214 amino acids ($SNX9_{214}$). Significantly, this region includes the complete SH3 domain of SNX9 (with the exception of 4 amino acids at the start) (Fig. 1B).

We assessed if binding of $SNX9_{214}$ to EspF was SH3 dependent. To this end we cloned the PCR fragment (using primers SNX9-ΔF and SNX9-R; Table 2) encoding $SNX9_{\Delta SH3}$ in the YTHS vector pGAD424 (generating plasmid pICC348) (Table 1). PJ69-4A cotransformed with pICC348 (expressing $SNX9_{\Delta SH3}$) and pICC175 (encoding EspF) did not grow on selective media or activate the β-galactosidase above a background level of enzymatic activity (Fig. 1A). These results show that in yeast SNX9-EspF protein interaction is mediated via the SH3 domain.

Interactions between recombinant EspF and SNX9 proteins. In order to confirm EspF-$SNX9_{214}$ protein interaction biochemically, the $SNX9_{214}$ cDNA clone was amplified by PCR using primers SNX9-F and SNX9-R and the fragment was cloned into pMAL-c2 (generating plasmid pICC351), for expression as an N-terminal maltose binding protein (MBP) fusion. *espF* was amplified by PCR using primers EspF-Fwd and EspF-Rev, and the fragment was cloned into pET28a (generating plasmid pICC350), for expression as an N-terminal His-tagged protein (His6). Purification of His-EspF and MBP-$SNX9_{214}$ was performed as described previously (10). A fusion protein of full-length SNX9 ($SNX9_{FL}$) fused to glutathione *S*-transferase (GST) was purified as described previously (15). We also used PCR to amplify a truncated version of $SNX9_{214}$ lacking the SH3 domain ($SNX9_{\Delta SH3}$) using primers SNX9-ΔF and SNX9R (Table 2). The PCR fragment was cloned into pMAL-c2 (generating plasmid pICC352). Overlaying His-EspF on nitrocellulose membranes containing MBP-$SNX9_{214}$

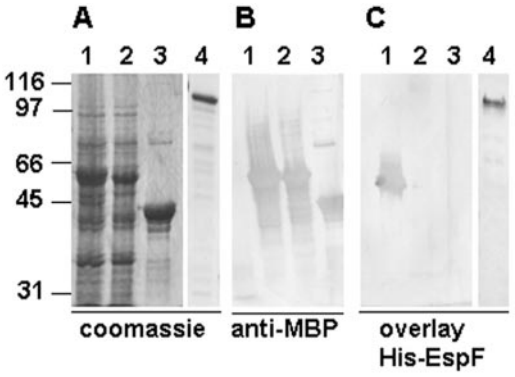

FIG. 2. EspF-SNX9$_{214}$ and EspF-SNX9$_{FL}$ protein interactions. Extracts of *E. coli* cell strains overexpressing MBP-SNX9$_{214}$ (lanes 1), MBP-SNX9$_{\Delta SH3}$ (lanes 2), MBP (lanes 3), and GST-SNX9$_{FL}$ (lanes 4) were separated on sodium dodecyl sulfate-polyacrylamide gels (A), transferred to nitrocellulose membranes, and probed with anti-MBP (B) or overlaid with His-EspF (C). Similar expression levels of MBP and GST protein derivatives are seen (A and B), but EspF bound specifically to MBP-SNX9$_{214}$ and GST-SNX9$_{FL}$ (C). Numbers at left are molecular masses in kilodaltons.

or MBP-SNX9$_{\Delta SH3}$, MBP, and GST-SNX9$_{FL}$ revealed specific binding only to the MBP-SNX9$_{214}$ and SNX9$_{FL}$ fusions (Fig. 2C).

EspF and SNX9 interact in EPEC-infected cells. EPECΔ*espF* (ICC175) was constructed using a modification of the λ Red recombinase method (4). Primers Δesp-F and ΔespF-R (Table 2) were used to amplify a Kan cassette, the PCR product was transformed into E2348/69(pKD46), and recombinant strains were selected on selective medium before pKD46 was cured by growth at 42°C. The mutation in *espF* was confirmed by PCR and DNA sequencing.

Wild-type (wt) EPEC and EPECΔ*espF* were used to infect HAC-7 cells. The cells were cultured in Dulbecco modified Eagle medium-10% fetal calf serum, infected at a multiplicity of infection of 100, incubated for 3.5 h, and mechanically fractionated into membrane and cytoplasmic fractions according to the method of Gauthier et al. (7). Employing polyclonal anti-SNX9$_{214}$ and anti-EspF rabbit antisera on Western blots revealed that EspF was detected at 20.9 kDa in membrane and cytoplasmic extracts of cells infected with wt EPEC but was not detected in either fraction prepared from cells infected with EPECΔ*espF* (Fig. 3A, upper panel). In contrast, SNX9 was detected as a 52-kDa band in cell extracts infected with either wt or EPECΔ*espF* strains (Fig. 3A, lower panel).

Coimmunoprecipitation (co-IP) was performed on the membrane and cytoplasmic extracts, which were precleared with immobilized protein A before IP. EspF and SNX9 were immunoprecipitated from EPEC-infected HeLa cell extracts in RIPA buffer (1% [vol/vol] Triton X-100; 50 mM Tris-HCl, pH 7.6; 400 μM $NaVO_4$; 100 g ml^{-1} phenylmethylsulfonyl fluoride; 10 mM leupeptin) with either polyconal anti-EspF or anti-SNX9$_{214}$ antibodies and immobilized protein A (Life Technologies, United Kingdom). The anti-EspF precipitates were resolved using sodium dodecyl sulfate-polyacrylamide gel electrophoresis, transferred to polyvinylidene difluoride membranes, and probed with anti-SNX9$_{214}$ (Fig. 3B, upper panel). The reverse IP of this experiment was also performed by precipitating extracts with anti-SNX9$_{214}$ and probing with anti-EspF (Fig. 3B, lower panel). EspF coprecipitates SNX9 from membrane extracts of HAC-7 cells infected with wt EPEC (Fig. 3B, upper panel, lane 2); no co-IP was observed in the equivalent cytoplasmic extracts (Fig. 3B, upper panel, lane 1). There was also no co-IP in membrane or cytoplasmic extracts of cells infected with EPECΔ*espF* (Fig. 3B, upper panel, lanes 3 and 4). In the reverse experiment, SNX9 coprecipitated EspF from membrane extracts infected with wt EPEC (Fig. 3B, lower panel, lane 1); no co-IP could be observed in the equivalent cytoplasmic extracts (Fig. 3B, lower panel, lane 2). Again there was also no co-IP in membrane or cytoplasmic extracts of cells infected with EPECΔ*espF* (Fig. 3B, lower panel, lanes 3 and 4). These results suggest that, following translocation, EspF binds SNX9 and that the complex is associated with the membrane fraction.

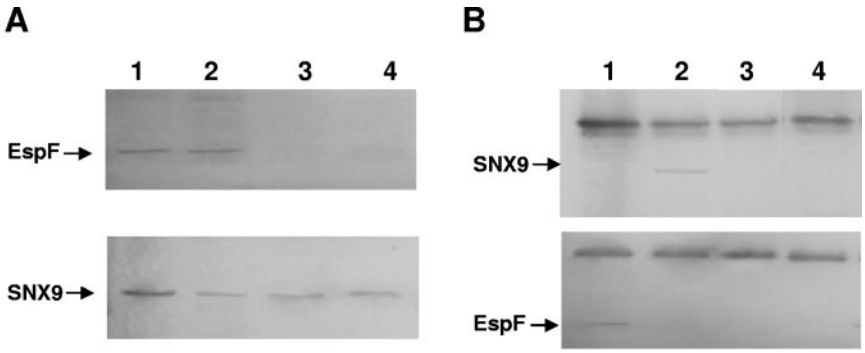

FIG. 3. A. Detection of EspF and SNX9 in membrane and cytoplasmic fractions of HAC-7 cells infected with wt EPEC (lanes 1 and 2) and EPECΔ*espF* (lanes 3 and 4). EspF was detected in both fractions only after infection with wt EPEC. SNX9 was detected in both cell fractions regardless of the EPEC strain used for infection. B. (Upper panel) IP with anti-EspF and detection with anti-SNX9, using membrane (lanes 2 and 4) and cytoplasmic (lanes 1 and 3) extracts of HAC-7 cells infected with wt EPEC (lanes 1 and 2) or EPECΔ*espF* (lanes 3 and 4). SNX9 was specifically coimmunoprecipitated with EspF from the membrane extract infected with wt EPEC (lane 2) but not with EPECΔ*espF*. (Lower panel) IP with anti-SNX9 and detection with anti-EspF, using membrane (lanes 1 and 3) and cytoplasmic (lanes 2 and 4) extracts of HAC-7 cells infected with wt EPEC (lanes 1 and 2) or EPECΔ*espF* (lanes 3 and 4). EspF was specifically coimmunoprecipitated with SNX9 from the membrane extract infected with wt EPEC (lane 1) but not with EPECΔ*espF*.

EspF and SNX9 colocalize in infected cells. EspF has previously been shown to be targeted to host cell mitochondria (21, 22). In this study we performed a time course examination of EspF translocation into HeLa cells and colocalized EspF and SNX9 in HeLa cells infected with "primed" wt EPEC strain E2348/69 bacteria (1:50 dilution of an overnight Luria broth culture grown for 2 h in Dulbecco modified Eagle medium) for up to 2 h at 37°C. The monolayers were washed three times in phosphate-buffered saline (PBS) to remove nonadhering bacteria and fixed in 4% buffered formalin. Washed monolayers were permeabilized with 0.2% Triton X-100 for 5 min, washed in PBS, and placed in blocking buffer (PBS-0.2% bovine serum albumin [BSA]). Cells were stained with rabbit polyclonal EspF antiserum (21) and $SNX9_{214}$ antiserum (1:100 in PBS-0.2% BSA) for 45 min at room temperature, washed three times in PBS, and counterstained with either Alexa 488 (green) or Alexa 594 (red) secondary antibody conjugates (Molecular Probes) diluted 1:50 in PBS-0.2% BSA for 45 min. For SNX9-EspF colocalization studies cells were first stained with SNX9 and Alexa 488 to saturation followed by EspF and Alexa 594 staining. Tetramethyl rhodamine isocyanate-conjugated phalloidin (5 μg/ml) (Sigma) was used to stain cell actin (red), and cells loaded with Mitotracker Red 580 (200 nM) (Molecular Probes) were used to stain cell mitochondria. Cells were mounted in CitiFluor mountant medium (Agar Scientific), and fluorescence imaging was performed using a Leica TCS SPII spectral confocal microscope. A transmitted light detector and phase contrast were used to image bacteria.

EspF was first detected inside cells beneath microcolonies of adherent bacteria (identified by actin accretion and phase contrast [not shown]) after 10 min (Fig. 4). By 20 to 30 min EspF was still detected beneath bacterial microcolonies but also in adjacent filamentous organelles (Fig. 4); comparison with cells stained with Mitotracker confirmed these organelles as mitochondria (data not shown). By 2 h most translocated EspF appeared in mitochondria (Fig. 4). No EspF staining was detected when cells were infected with EPECΔ*espF* (Fig. 4). These observations indicate an initial cytosolic localization of EspF followed by rapid translocation to mitochondria.

To visualize the EspF-SNX9 complex during infection, we performed colocalization studies. Uninfected cells and cells infected for 1 h with E2348/69 were stained first for SNX9 and then for EspF. In uninfected cells SNX9 had a punctate distribution but was mainly concentrated around the cell periphery; there was no EspF staining (Fig. 4). In contrast, following EPEC infection, SNX9 became focused beneath bacterial microcolonies. Double staining of SNX9 and EspF revealed colocalization of SNX9 and EspF beneath bacterial microcolonies whereas EspF that had migrated to mitochondria did not colocalize with SNX9 (Fig. 4).

SNX9 is implicated in the clathrin endocytic pathway (15). We therefore examined the distribution of clathrin in uninfected cells and cells infected with wt E2348/69 and EPECΔ*espF*, using mouse monoclonal clathrin antiserum (Sigma). Clathrin was present throughout uninfected HeLa cells but concentrated in perinuclear regions, and this distribution of clathrin was unchanged following a 2-h infection with E2348/69 (Fig. 5) and EPECΔ*espF* (data not shown); no clathrin became concentrated beneath the microcolonies of adherent bacteria (Fig. 5). These results indicate that SNX9-EspF interaction is probably

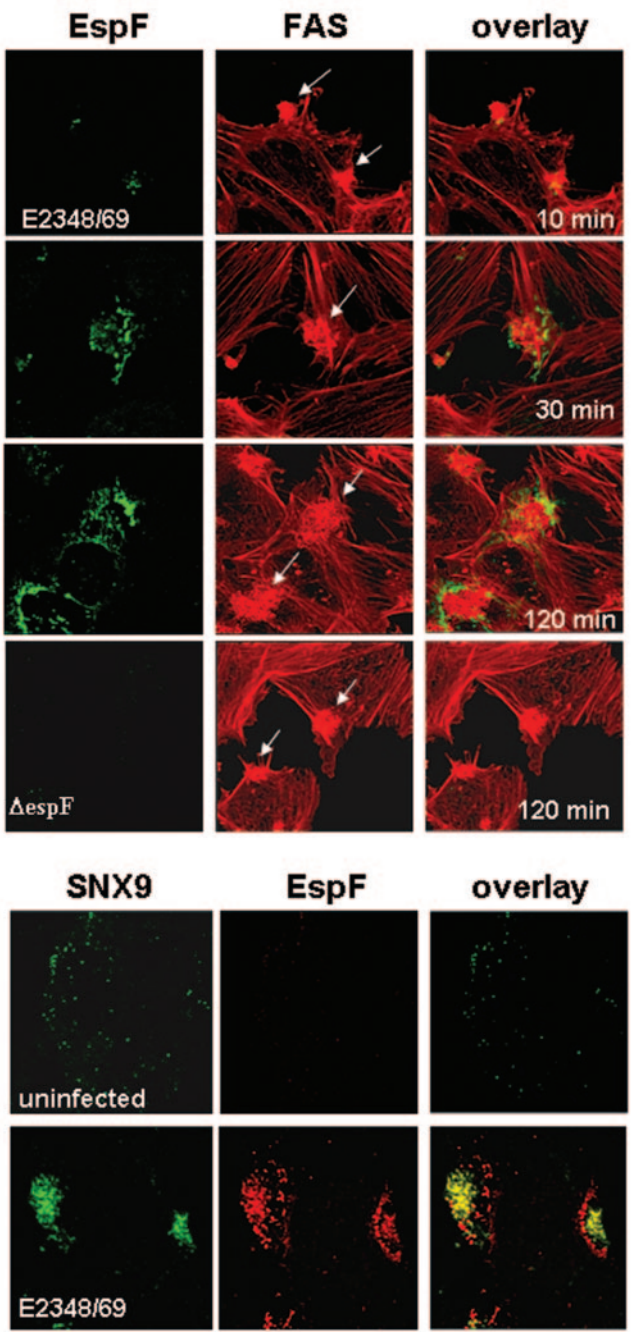

FIG. 4. (Top) Translocation of EspF into HeLa cells. Confocal images show HeLa cells infected for 10, 30, and 120 min with primed cultures of wt E2348/69 and for 120 min with an *espF* mutant. Cells were stained for EspF and cell actin. EspF was detected beneath bacterial microcolonies (sites of actin accretion, arrows) after 10 min, but by 30 min EspF staining was also seen in adjacent filamentous organelles identified as mitochondria; after 2 h staining was predominantly in mitochondria. The *espF* mutant induced actin accretion but did not translocate EspF. (Bottom) Colocalization of SNX9 and EspF. Confocal images show uninfected HeLa cells and cells infected for 1 h with E2348/69 and stained for SNX9 and EspF. A punctate distribution of SNX9 was seen in uninfected cells, but following EPEC infection SNX9 became concentrated beneath bacterial colonies and colocalized with EspF (overlay, yellow); EspF that had migrated to adjacent mitochondria did not colocalize with SNX9 (overlay, red).

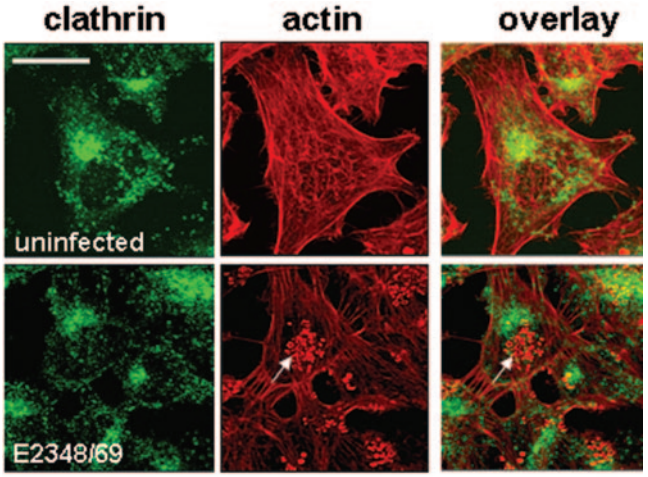

FIG. 5. Localization of clathrin. Confocal images show uninfected HeLa cells and cells infected for 1 h with E2348/69 and stained for clathrin and cell actin. Clathrin was seen throughout the cell, but concentrations were frequently seen in a perinuclear region of the cell. This distribution was unchanged following EPEC infection, and there was no clathrin accumulation beneath sites of bacterial adhesion (arrow). Bar = 5 μm.

unrelated to clathrin distribution. Indeed, we observed no difference in clathrin-mediated endocytosis of transferrin following infection of HeLa-2 cells with either wt EPEC or EPEC Δ*espF* strains (data not shown).

Concluding remarks. The SNX family of hydrophilic proteins is characterized by the presence of a Phox homology, phospholipid-binding domain (28). In addition, SNXs contain various protein-protein interaction motifs. Among the 25 human SNXs that have been identified thus far, only SNX9 and SNX18 contains an SH3 domain. Indeed, $EspF_{EPEC}$ contains three proline-rich repeats (18), and in this study we have shown that the interaction between SNX9 and EspF is mediated by the SNX9 SH3 domain.

Translocation assays have shown that at 10 min after infection of HeLa cells EspF was detected beneath bacterial microcolonies at sites of actin accretion. By 30 min EspF staining was also seen in adjacent filamentous organelles identified as mitochondria, while after 2 h staining was predominantly in mitochondria. Using co-IP we have shown that EspF specifically interacts with membrane-bound SNX9; no co-IP was detected with the cytosolic fraction of SNX9. This result is consistent with the observation that following infection SNX9 is focused and colocalized with EspF at the site of attached EPEC microcolonies; there was no colocalization of SNX9 with cytosolic or mitochondrion-associated EspF. SNX9 has an accessory role in the endocytic processes as it binds clathrin, the adaptor protein 2, and Cdc42-associated tyrosine kinase 2, which are involved in formation of clathrin-coated vesicles and endocytosis (28). In this study we found that the distribution of clathrin was not significantly different between uninfected, wt EPEC-infected and EPEC Δ*espF*-infected cells. As such, although by using several complementary biochemical and cellular approaches we confirmed that EspF binds SNX9, we were unable to attribute a function to the EspF-SNX9 complex during EPEC infection; defining the role of the complex will be the subject of future investigations.

This project was supported by the Wellcome Trust. O. Marchès is supported by a Marie Curie fellowship from the European Commission.

REFERENCES

1. **Batchelor, M., J. Guignot, A. Patel, N. Cummings, J. Cleary, S. Knutton, D. W. Holden, I. Connerton, and G. Frankel.** 2004. Involvement of the intermediate filament protein cytokeratin-18 in actin pedestal formation during EPEC infection. EMBO Rep. **5:**104–110.
2. **Crane, J. K., B. P. McNamara, and M. S. Donnenberg.** 2001. Role of EspF in host cell death induced by enteropathogenic *Escherichia coli*. Cell. Microbiol. **3:**197–211.
3. **Creasey, E. A., R. M. Delahay, S. J. Daniell, and G. Frankel.** 2003. Yeast two-hybrid system survey of interactions between LEE-encoded proteins of enteropathogenic *Escherichia coli*. Microbiology **149:**2093–2106.
4. **Datsenko, K. A., and B. L. Wanner.** 2000. One-step inactivation of chromosomal genes in *Escherichia coli* K12 using PCR products. Proc. Natl. Acad. Sci. USA **97:**6640–6645.
5. **Frankel, G., A. D. Phillips, L. R. Trabulsi, S. Knutton, G. Dougan, and S. E. Matthews.** 2001. Intimin and the host cell—is it bound to end in Tir(s)? Trends Microbiol. **9:**214–218.
6. **Garmendia, J., G. Frankel, and V. F. Crepin.** 2005. Enteropathogenic and enterohemorrhagic *Escherichia coli* infections: translocation, translocation, translocation. Infect. Immun. **73:**2573–2585.
7. **Gauthier, A., M. de Grado, and B. B. Finlay.** 2000. Mechanical fractionation reveals structural requirements for enteropathogenic *Escherichia coli* Tir insertion into host membranes. Infect. Immun. **68:**4344–4348.
8. **Goosney, D. L., R. DeVinney, and B. B. Finlay.** 2001. Recruitment of cytoskeletal and signaling proteins to enteropathogenic and enterohemorrhagic *Escherichia coli* pedestals. Infect. Immun. **69:**3315–3322.
9. **Hardwidge, P. R., W. Deng, B. A. Vallance, I. Rodriguez-Escudero, V. J. Cid, M. Molina, and B. B. Finlay.** 2005. Modulation of host cytoskeleton function by the enteropathogenic *Escherichia coli* and *Citrobacter rodentium* effector protein EspG. Infect. Immun. **73:**2586–2594.
10. **Hartland, E. L., M. Batchelor, R. M. Delahay, C. Hale, S. Matthews, G. Dougan, S. Knutton, I. Connerton, and G. Frankel.** 1999. Binding of intimin from enteropathogenic *Escherichia coli* to Tir and to host cells. Mol. Microbiol. **32:**151–158.
11. **Kenny, B., R. DeVinney, M. Stein, D. J. Reinscheid, E. A. Frey, and B. B. Finlay.** 1997. Enteropathogenic *E. coli* (EPEC) transfers its receptor for intimate adherence into mammalian cells. Cell **91:**511–520.
12. **Kenny, B., S. Ellis, A. D. Leard, J. Warawa, H. Mellor, and M. A. Jepson.** 2002. Co-ordinate regulation of distinct host cell signalling pathways by multifunctional enteropathogenic *Escherichia coli* effector molecules. Mol. Microbiol. **44:**1095–1107.
13. **Knutton, S., T. Baldwin, P. H. Williams, and A. S. McNeish.** 1989. Actin accumulation at sites of bacterial adhesion to tissue culture cells: basis of a new diagnostic test for enteropathogenic and enterohemorrhagic *Escherichia coli*. Infect. Immun. **57:**1290–1298.
14. **Knutton, S., D. R. Lloyd, and A. S. McNeish.** 1987. Adhesion of enteropathogenic *Escherichia coli* to human intestinal enterocytes and cultured human intestinal mucosa. Infect. Immun. **55:**69–77.
15. **Lundmark, R., and S. R. Carlsson.** 2003. Sorting nexin 9 participates in clathrin-mediated endocytosis through interactions with the core components. J. Biol. Chem. **278:**46772–46781.
16. **Matsuzawa, T., A. Kuwae, S. Yoshida, C. Sasakawa, and A. Abe.** 2004. Enteropathogenic *Escherichia coli* activates the RhoA signaling pathway via the stimulation of GEF-H1. EMBO J. **23:**3570–3582.
17. **McDaniel, T. K., K. G. Jarvis, M. S. Donnenberg, and J. B. Kaper.** 1995. A genetic locus of enterocyte effacement conserved among diverse enterobacterial pathogens. Proc. Natl. Acad. Sci. USA **92:**1664–1668.
18. **McNamara, B. P., and M. S. Donnenberg.** 1998. A novel proline-rich protein, EspF, is secreted from enteropathogenic *Escherichia coli* via the type III export pathway. FEMS Microbiol. Lett. **166:**71–78.
19. **McNamara, B. P., A. Koutsouris, C. B. O'Connell, J. P. Nougayrede, M. S. Donnenberg, and G. Hecht.** 2001. Translocated EspF protein from enteropathogenic *Escherichia coli* disrupts host intestinal barrier function. J. Clin. Investig. **107:**621–629.
20. **Miller, J. H.** 1972. Experiments in molecular genetics. Cold Spring Harbor Laboratory, Cold Spring Harbor, N.Y.
21. **Nagai, T., A. Abe, and C. Sasakawa.** 2004. Targeting of enteropathogenic *Escherichia coli* EspF to host mitochondria is essential for the bacterial pathogenesis: critical role of the 16th leucine residue in EspF. J. Biol. Chem. **280:**2998–3011.
22. **Nougayrede, J. P., and M. S. Donnenberg.** 2004. Enteropathogenic *Escherichia coli* EspF is targeted to mitochondria and is required to initiate the mitochondrial death pathway. Cell. Microbiol. **6:**1097–1111.

23. **Shaw, R. K., J. Cleary, G. Frankel, and S. Knutton.** 2005. Enteropathogenic *Escherichia coli* interaction with human intestinal mucosa: role of effector proteins in brush border remodeling and formation of attaching and effacing lesions. Infect. Immun. **73:**1243–1251.
24. **Shaw, R. K., K. Smollett, J. Cleary, J. Garmendia, A. Straatman-Iwanowska, G. Frankel, and S. Knutton.** 2005. Enteropathogenic *E. coli* type III effectors EspG and EspG2 disrupt the microtubule network of intestinal epithelial cells. Infect. Immun. **73:**4385–4390.
25. **Tomson, F. L., V. K. Viswanathan, K. J. Kanack, R. P. Kanteti, K. V. Straub, M. Menet, J. B. Kaper, and G. Hecht.** 2005. Enteropathogenic *Escherichia coli* EspG disrupts microtubules and in conjunction with Orf3 enhances perturbation of the tight junction barrier. Mol. Microbiol. **56:** 447–464.
26. **Tu, X., I. Nisan, C. Yona, E. Hanski, and I. Rosenshine.** 2003. EspH, a new cytoskeleton-modulating effector of enterohaemorrhagic and enteropathogenic *Escherichia coli*. Mol. Microbiol. **47:**595–606.
27. **Viswanathan, V. K., S. Lukic, A. Koutsouris, R. Miao, M. M. Muza, and G. Hecht.** 2004. Cytokeratin 18 interacts with the enteropathogenic *Escherichia coli* secreted protein F (EspF) and is redistributed after infection. Cell. Microbiol. **6:**987–997.
28. **Worby, C. A., and J. E. Dixon.** 2002. Sorting out the cellular functions of sorting nexins. Nat. Rev. Mol. Cell Biol. **3:**919–931.